Electronic Supplementary Information

Electrochemiluminescence immunosensor using poly(L-histidine) protected glucose dehydrogenase on Pt/Au bimetallic nanoparticles to in situ generate co-reactant

Lijuan Xiao, Yaqin Chai*, Haijun Wang and Ruo Yuan

Education Ministry Key Laboratory on Luminescence and Real-Time Analytical Chemistry, College of Chemistry and Chemical Engineering, Chongqing 400715, People's Republic of China

The preparation of 0.25 wt % chitosan solution

0.25 *wt* % chitosan solutions were prepared by dissolving 25 mg chitosan in 10 mL 1% acetic acid solution with magnetic stirring for ~2 h.

The preparation of AuNPs

AuNPs were synthesized according to the previous report with a little modification[1]. Briefly, 1.0 mL of 1% HAuCl4 was diluted into 100.0 mL with double-distilled water and brought to reflux while stirring. Subsequently, 4.0 mL of 1% trisodium citrate solution was added quickly, resulting in a color change from pale yellow to wine red. After that, the solution was refluxed for another 15 min.

The Characterization of the Au@RuSiO$_2$ NPs

* Corresponding author. Tel.: +86-23-68252277; Fax: +86-23-68253172.

E-mail address: yqchai@swu.edu.cn (Y. Q. Chai)

Fig. S2A showed the UV-vis absorption spectra of Au NPs, $Ru(phen)_3^{2+}$, $RuSiO_2$ NPs, $Au@RuSiO_2$ NPs, respectively. Obviously, the absorbance peak of Au NPs colloid was appeared at 520 nm (Fig. S2A (a)). $Ru(phen)_3^{2+}$ exhibited there characteristic peaks at 447 nm, 281 nm and 222 nm (Fig. S2A (b)). The synthesized $RuSiO_2$ NPs had similar peaks (Fig. S2A (c)), suggesting that many $Ru(phen)_3^{2+}$ molecules were doped into SiO_2 NPs successfully through the electrostatic interaction between $Ru(phen)_3^{2+}$ and silica nanoparticles. After that, Au NPs were assembled onto the $RuSiO_2$ NPs surfaces with the aid of BSA. The spectrum of $Au@RuSiO_2$ NPs shows the characteristic absorption peaks of Au NPs and $RuSiO_2$ NPs (Fig. S2A (d)), indicating the $Au@RuSiO_2$ NPs were prepared successfully.

In addition, scanning electron microscopy (SEM) was also used to characterize the synthesis of $Au@RuSiO_2$ NPs. As shown in Fig. S2B, the $RuSiO_2$ NPs were well-dispersed particles with a uniform diameter of ~150 nm, which were much larger than Au NPs, thus mangy Au NPs can load on $RuSiO_2$ NPs to form $Au@RuSiO_2$ NPs. Fig. S2C shown that the $RuSiO_2$ NPs were covered with a great deal of small spherical Au NPs, which demonstrated that the $Au@RuSiO_2$ NPs were prepared successfully.

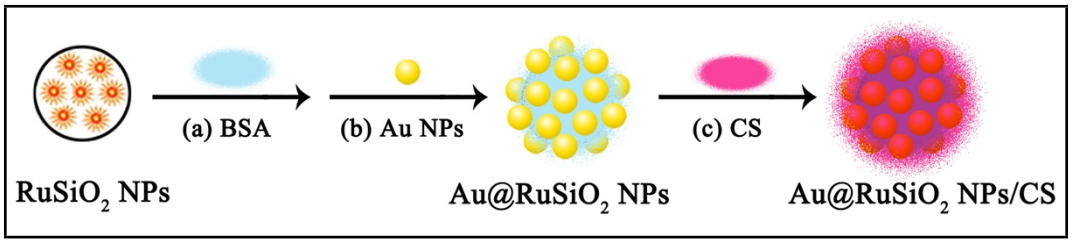

Fig. S1 Preparation procedures of $Au@RuSiO_2$ NPs/CS.

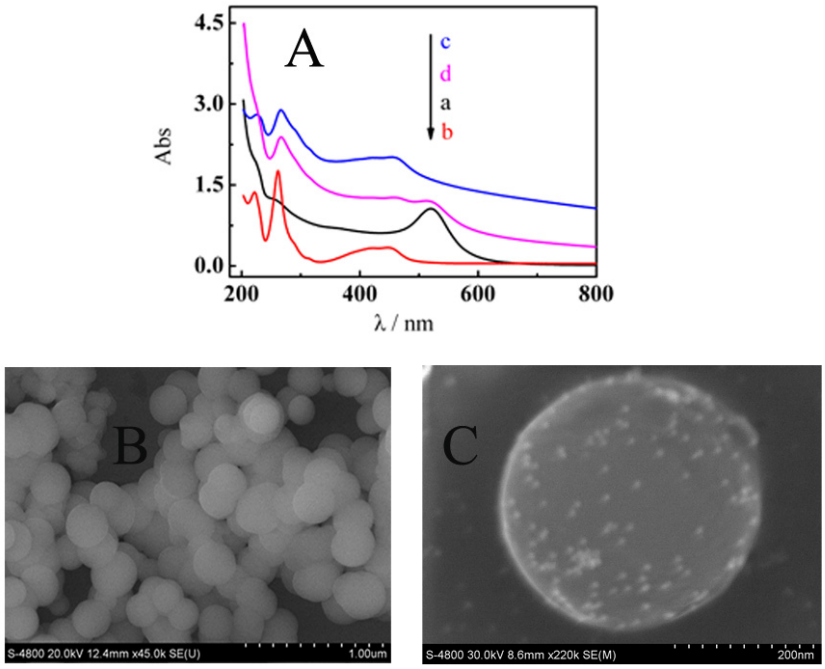

Fig. S2 (A) UV-vis spectra of Au NPs (a, black), $Ru(phen)_3^{2+}$ (b, red), $RuSiO_2$ NPs (c, blue), $Au@RuSiO_2$ NPs (d, magenta), (B) SEM images of $RuSiO_2$ NPs and (C) SEM images of $Au@RuSiO_2$ NPs.

CV Characterization of the immunosensor fabrication

To gain a better understanding of the fabrication process, the cyclic voltammograms (CVs) experiments were also performed in 5 mM $[Fe(CN)_6]^{3-/4-}$ solution. As shown in Fig. S3, a pair of well-defined redox peak of $[Fe(CN)_6]^{3-/4-}$ was observed on the pretreated bare GCE (curve a). When $Au@RuSiO_2$ NPs/CS complex were dropped onto the electrode, the current decreased clearly due to the insulating properties of CS (curve b). After the successive immobilization of Ab_1, BSA and cTnI, the peak current further decreased in order (curve c, d and e). That was because the formation of protein molecules layers hindered the electron transfer.

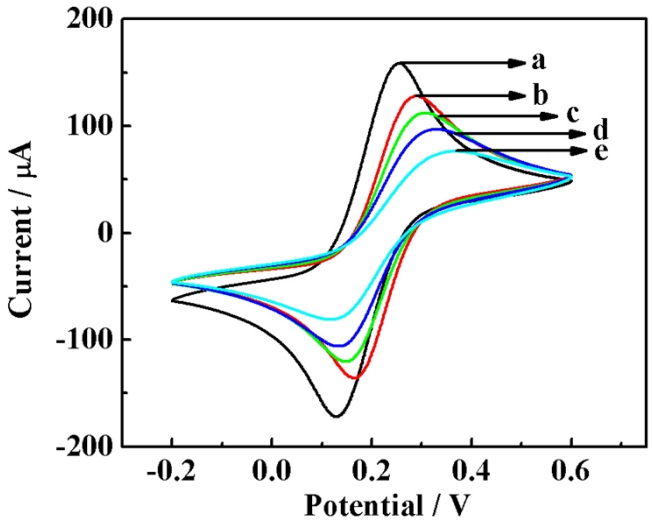

Fig. S3 CV for (a) bare GCE, (b) Au@RuSiO$_2$ NPs/CS/GCE, (c) Ab$_1$/Au@RuSiO$_2$ NPs/CS/GCE, (d) BSA/Ab$_1$/Au@RuSiO$_2$ NPs/CS/GCE, (e) cTnI/BSA/Ab$_1$/Au@RuSiO$_2$ NPs /CS/GCE, (f) Pt/Au NPs@GDH-PLH-Ab$_2$/cTnI/BSA/Ab$_1$/Au@RuSiO$_2$ NPs/CS/GCE, in 0.1 M KCl solution containing 5 mM $[Fe(CN)_6]^{3-/4-}$. Scan rate, 100 mV s^{-1}.

Comparisons of proposed immunosensor with other detection methodologies for cTnI detection

Table S1 Performance compared with other detection methodologies for cTnI detection.

Detection method	Linear range/ng mL^{-1}	Detection limit/pg mL^{-1}	Ref.
Surface Acoustic Wave	0.02 ~ 100	20	2
Surface Plasmon Resonance	0.03 ~ 6.5	10	3
Surface Plasmon Resonance	0.05 ~ 4.5	50	4
Localized Surface Plasmon Resonance	1 ~ 20	300	5
Electrochemiluminescent	0.01 ~ 5	4.5	6
Electrochemiluminescent	0.01 ~ 10	3.33	Our work

From the Table S1 we can see that the proposed immunosensor has a relative large linear range and low detection limit compared with previous reports.

Reference

1 G. Frens, *Nature,* 1973, **241,** 20.

2 J. Lee, Y.S. Choi, Y. Lee, H.J. Lee, J.N. Lee, S.K. Kim, K.Y. Han, E.C. Cho, J.C. Park and S.S. Lee, *Anal. Chem.,* 2011, **83,** 8629.

3 F. Dutra and L.T. Kubota, *Clin. Chim. Acta,* 2007, **376,** 114.

4 R.F. Dutra, R.K. Mendes, V. Lins da Silva and L.T. Kubota, *J. Pharm. Biomed. Anal.,* 2007, **43,** 1744.

5 L. Tang, J. Casas and M. Venkataramasubramani, *Anal. Chem.,* 2013, **85,** 1431.

6 H.L. Qi, X.Y. Qiu, D.P. Xie, C. Ling, Q. Gao and C.X. Zhang, *Anal. Chem.,* 2013, **85,** 3886.